Flow of a Bingham fluid in a non symmetric inclined channel

Flow of a Bingham Fluid in a non Symmetric Inclined Channel

Lorenzo Fusi[a,*], Angiolo Farina[a]

[a]*Università degli Studi di Firenze*
Dipartimento di Matematica e Informatica "Ulisse Dini"
Viale Morgagni 67/a, 50134 Firenze, Italy

Abstract

The flow of a Bingham fluid in a tilted channel of non uniform width is considered. The upper wall of the channel is assumed to be flat but not parallel to the bottom one and the flow is driven by the gravity. A lubrication approximation is considered and an analytical solution is determined. We find conditions ensuring the appearance of the plug at a certain distance from the channel inlet. We also give an explicit formula for the pressure drop along the channel. Some numerical simulations are worked out for different values of the Bingham number and for different slopes of the upper wall.

Keywords: Bingham fluid, Lubrication theory, Asymptotic expansion, Numerical simulations

1. Introduction

Viscoplastic fluids are characterized by the absence of deformations when the applied load is below a fixed threshold. Bingham fluids are a special class of Viscoplatic fluids named so after Bingham [3], [4], who described several types of paint using this definition. Viscoplastic fluids constitute a very important class of non-Newtonian fluids.

The modelling of Bingham materials is of crucial importance in industrial applications, since a large variety of materials (e.g. foams, pastes, slurries, oils, ceramics, etc.) exhibit the fundamental character of viscoplasticity, that is the capability of flowing only if the stress is above some critical value.

Though the constitutive models (especially within the framework of implicit constitutive theory [21], [23], [24]) appear to be quite simple, the flow of these materials is difficult to predict, especially because of the presence of unknown interfaces separating the yielded and the unyielded regions which are difficult to track, [2]. This is particularly evident when the flow occurs in complex geometries and even when major simplifications, such as lubrication approximation, can be applied. In some cases the Bingham model may lead to a paradox, known as the "lubrication paradox", which contradicts the assumption of a truly unyielded phase, [17], [6], [20], [25] and [12].

During the last decades many different studies have been carried out to explain the paradox. Walton and Bittleston [26], who studied the axial flow in an eccentric annular duct, for instance, proved that a true plug exists in the middle of the channel on both the wide and narrow part of the annulus, with a pseudo-plug placed between the two rigid zones. Balmforth and Craster [1] and subsequently Frigaard and Ryan [6] developed asymptotic procedures that allow to overcome the lubrication paradox and build a consistent solution for thin layer flows. As shown in [20], the paradox can indeed be resolved by considering higher order terms of the lubrication expansion which shows that actually the plugs are slightly above the yield stress (pseudo plugs in which true rigid plugs are embedded). Recently Muravleva [18] has studied the planar squeeze flow of a Bingham fluid, exploiting the asymptotic technique introduced in [1] determining intact true plug regions and overcoming thus the lubrication paradox.

An interesting approach for circumventing the paradox consists in the use of regularization procedures that regularize the effective viscosity, as the bi-viscous model adopted in [27], [14]. Another way to smooth the singularities arising from the classical viscoplastic models is to take into account possible deformations of the plug, a procedure first suggested by Oldroyd [19]. Regarding the latter approach, the authors have carried out in the last ten years a series of papers in which they have relaxed the hypothesis of a perfectly rigid unyielded region assuming that the plug may undergo elastic deformations [7], [8] [9], [10], [11], [12].

Recently, in [15], [16], Fusi et al. have proposed a new methodology to investigate the motion of unyielded part of a viscoplastic fluid. With this procedure the authors were able to overcome the paradox at the leading order of the lubrication scaling.

In this new approach the unyielded part is modelled as an evolving non material volume, whose motion is determined only by the stress applied by the fluid that surrounds the unyielded plug. Momentum balance is then written using an integral formulation where only the external stresses acting on the boundary are required.

The main advantage of this procedure is that no assumption must be made on the order of magnitude of the stress when applying the lubrication scaling. This is clearly useful, since, within the unyielded domain, the Cauchy stress is "indeterminate" and we cannot identify (neither a priori nor a posteriori)

*Corresponding author: tel. +39552751437, Fax +39552751452
Email address: fusi@math.unifi.it (Lorenzo Fusi)

which term can be disregarded when the scaling is applied. This approach has proved successful, allowing to determine a velocity field of the unyielded phase that does not depends on the spatial coordinates (no lubrication paradox).

In this paper we use the procedure introduced in [15], [16], to investigate the downhill motion of a Bingham fluid in a non symmetric inclined channel: the upper wall of the channel is assumed to be flat but not parallel to the bottom wall (see Fig. 1). We study the dynamics of the flow supposing that gravity is the only driving force and we model the unyielded plug using an integral approach we developed in [15], [16]. We developed the model supposing that the local volumetric discharge is constant throughout the channel.

We prove that we can explicitly track the yield surfaces that separate the yielded from the unyielded domain and we find constraints that ensure that the flow never comes to a stop. In particular we find that the plug is placed between the walls and expands as the channel narrows. We determine conditions which guarantees the existence of the plug throughout the channel. We also give an explicit formula for the calculation of the pressure drop. Finally in the Appendix, we provide a detailed mathematical analysis to prove the existence and uniqueness of the yield surfaces.

2. Mathematical modelling

In a Bingham fluid the Cauchy stress is given by[1] $\mathbf{T}^* = -P^*\mathbf{I} + \mathbf{S}^*$, with the deviatoric part given by

$$\mathbf{D}^* - \mathbf{S}^* \left[\frac{II_{\mathbf{D}^*}}{2\eta^* II_{\mathbf{D}^*} + \tau_o^*} \right] = 0, \tag{1}$$

where $\mathbf{D}^*$ is the symmetric part of the rate-of-strain tensor, η^* is a viscosity, τ_o^* the critical threshold for the stress invariant

$$II_{\mathbf{S}^*} = \sqrt{(2^{-1}\mathbf{S}^* \cdot \mathbf{S}^*)}$$

and

$$II_{\mathbf{D}^*} = \sqrt{(2^{-1}\mathbf{D}^* \cdot \mathbf{D}^*)}.$$

Equation (1) holds when $II_{\mathbf{S}^*} \geq \tau_o^*$, while $II_{\mathbf{D}^*} \equiv 0$ when $II_{\mathbf{S}^*} \leq \tau_o^*$. The shear stress-shear rate relation can be visualized writing $II_{\mathbf{S}^*}$ as a function of $II_{\mathbf{D}^*}$

$$II_{\mathbf{S}^*} = 2\eta^* II_{\mathbf{D}^*} + \tau_o^*, \tag{2}$$

We confine ourselves to a bi-dimensional setting like the one depicted in Fig. 1. In practice we consider the flow occurring in a channel of non uniform width over an inclined plane whose tilt angle is α. The velocity field is assumed to be of the form

$$\mathbf{u}^*(x^*, y^*, t^*) = u^*(x^*, y^*, t^*)\boldsymbol{e}_1 + v^*(x^*, y^*, t^*)\boldsymbol{e}_2 \, .$$

Referring again to Fig. 1, the flow domain is $0 < x^* \leq L^*$, $0 \leq y^* \leq h^*(x^*)$, where

$$h^*(x^*) = H^* - \tilde{A}\, x^*,$$

[1] Throughout the paper the starred quantities are dimensional.

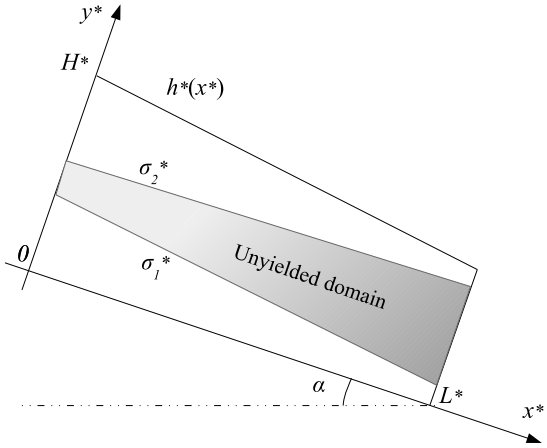

Figure 1: Flow down an inclined plane.

with $\tilde{A} > 0$ and $H^* - \tilde{A}\, L^* > 0$. The fluid domain is then divided in a plug region $[\sigma_1^*, \sigma_2^*]$ where $II_{\mathbf{S}^*} \leq \tau_o^*$ and two fluid regions $[0, \sigma_1^*]$, $[\sigma_2^*, h^*]$ where $II_{\mathbf{S}^*} \geq \tau_o^*$. Of course σ_1^* and σ_2^* are free boundaries that have to be determined. We assume that the characteristic longitudinal length is L^*, and we denote by H^* the transversal characteristic length, i.e. $H^* = h^*(0)$. The governing equations in the fluid region $[0, \sigma_1^*] \cup [\sigma_2^*, h^*]$ are

$$\rho^* \left(u_t^* + u_x^* u^* + u_y^* v^* \right) = \rho^* g^* \sin\alpha - P_x^* + (S_{11}^*)_x + (S_{12}^*)_y,$$

$$\rho^* \left(v_t^* + v_x^* u^* + v_y^* v^* \right) = -\rho^* g^* \cos\alpha - P_y^* + (S_{12}^*)_x + (S_{22}^*)_y,$$

where ρ^* is the material density, g^* is gravity (see again Fig. 1). Mass balance is expressed by

$$u_x^* + v_y^* = 0,$$

In the rigid domain $[\sigma_1^*, \sigma_2^*]$ the velocity field is the one of a rigid motion

$$\begin{cases} u^* = -\omega^*(t^*) y^* + k_1^*(t^*), \\ \\ v^* = \omega^*(t^*) x^* + k_2^*(t^*), \end{cases} \tag{3}$$

where $\omega^*(t^*)$ (angular velocity) and $k_j^*(t^*)$ are unknown. Following the approach introduced in [15] we write the linear momentum conservation in the rigid part in the integral form

$$\int_{\Omega_t^*} \rho^* \frac{d\mathbf{u}^*}{dt^*} d\mathbf{x}^* = \int_{\partial\Omega_t^*} (\mathbf{T}^*\mathbf{n}) d\sigma^* + \int_{\Omega_t^*} \rho^* \mathbf{f}^* d\mathbf{x}^*, \tag{4}$$

where d/dt^* is the material derivative and where

$$\Omega_t^* = \{(x^*, y^*) : \quad y^* \in (\sigma_1^*, \sigma_2^*), \quad x^* \in (0, L^*)\},$$

and

$$\mathbf{f}^* = g^* (\sin\alpha\, \boldsymbol{e}_1 - \cos\alpha\, \boldsymbol{e}_2),$$

represent the unyielded domain and the body force (gravity) respectively. We assume no-slip boundary conditions $\mathbf{u}^* = 0$ on $y^* = 0$ and $y^* = h^*$. We also assume that the volumetric flow rate on each cross section is constant so that

$$U^* H^* = \int_0^{h^*} u^*(x^*, y^*, t^*) dy^*. \tag{5}$$

3. Nondimensionalization

We assume that the ratio $\varepsilon = H^*/L^*$ is sufficiently small so that lubrication approximation applies. Following [13] we rescale the main variables of the problem in the following way

$$x^* = L^* x, \quad y^* = \varepsilon L^* y, \quad u^* = U^* u, \quad v^* = \varepsilon U^* v,$$

$$h^* = H^* h, \quad \sigma_1^* = H^* \sigma_1, \quad \sigma_2^* = H^* \sigma_2,$$

$$k_1^* = U^* k_1, \quad k_2^* = \varepsilon U^* k_2, \quad \omega^* = \left(U^* H^{*^{-1}}\right) \omega$$

where U^* is the characteristic longitudinal velocity given by (see [5])

$$U^* = \frac{H^{*^2} \rho^* g^* \sin\alpha}{\eta^*}. \tag{6}$$

Moreover

$$\mathbf{D}^* = \left(\frac{U^*}{H^*}\right)\mathbf{D}, \quad II_{\mathbf{D}^*} = \left(\frac{U^*}{H^*}\right) II_{\mathbf{D}}, \quad P^* = \left(\frac{\eta^* U^* L^*}{H^{*^2}}\right) P,$$

$$\mathbf{S}^* = \left(\frac{\eta^* U^*}{H^*}\right) S, \qquad II_{\mathbf{S}^*} = \left(\frac{\eta^* U^*}{H^*}\right) II_{\mathbf{S}},$$

Remark 1. *Recalling (6), we notice that the characteristic pressure can also be expressed as*

$$\frac{\eta^* U^* L^*}{H^{*^2}} = \rho^* g^* L^* \sin\alpha.$$

We introduce the nondimensional numbers[2]

$$\mathsf{Re} = \frac{\rho^* U^* H^*}{\eta^*}, \qquad \mathsf{Bi} = \left(\frac{\tau_o^* H^*}{\eta^* U^*}\right), \qquad \theta = \frac{\varepsilon}{\tan\alpha}, \qquad A = \frac{\tilde{A}}{\varepsilon}.$$

We assume $\tilde{A} = O(\varepsilon)$ and require $A < 1$, so that the bottom and upper plates are always detached. Hence

$$A \in [0, 1). \tag{7}$$

We can reformulate the problem in the non dimensional form

$$\begin{cases} \varepsilon \mathsf{Re}\left(u_t + u_{1x} u_1 + u_y v\right) = 1 - P_x + \varepsilon (S_{11})_x + (S_{12})_y, \\ \varepsilon^3 \mathsf{Re}\,(v_t + v_x u + v y v) = -\theta - P_y + \varepsilon^2 (S_{12})_x + \varepsilon (S_{22})_y, \\ u_x + v_y = 0, \end{cases} \tag{8}$$

where

$$\mathbf{S} = \left(2 + \frac{\mathsf{Bi}}{II_{\mathbf{D}}}\right)\mathbf{D}. \tag{9}$$

The non dimensional equation of the upper plate becomes $h(x) = 1 - Ax$. In the unyielded domain

$$\begin{cases} u = -\omega(t) y + k_1(t), \\ \varepsilon^2 v = \omega(t) x + \varepsilon^2 k_2(t). \end{cases} \tag{10}$$

[2] Re and Bi are the Reynolds and Bingham number respectively.

Remark 2. *In (10) we have rescaled the angular velocity ω^* with $U^* H^{-1}$. This choice comes from the following observation. Angular velocity ω^* is found writing the non zero components of the spin tensor*

$$\omega^* = \frac{1}{2}\left(\frac{\partial u^*}{\partial y^*} - \frac{\partial v^*}{\partial x^*}\right),$$

so that

$$\omega^* = \frac{U^*}{2H^*}\left(\frac{\partial u}{\partial y} - \varepsilon^2 \frac{\partial v}{\partial x}\right).$$

Assuming that all the derivatives are $O(1)$, we find that the characteristic angular velocity is $U^* H^{*^{-1}}$. The scaling of (3) with the characteristic angular velocity $U^* H^{*^{-1}}$ provides (10).

Actually the angular velocity ω^* vanishes, as we shall see from formula (29). Indeed, as rule of thumb, we know that $\omega^* = U^* \varkappa^*$, where $\varkappa^*$ is the curvature radius of the channel. Since the channel is essentially flat, $\varkappa^* \to 0$, and $\omega^* \to 0$.

Following [15] we see that the first component of equation (4) can be rewritten as

$$\mathsf{Re}\varepsilon\left(\int_0^1 dx \int_{\sigma_1}^{\sigma_2} \frac{du}{dt} dy\right) = \int_{\sigma_1(0)}^{\sigma_2(0)} (P - \varepsilon S_{11})|_0 \, dy +$$

$$- \int_{\sigma_1(1)}^{\sigma_2(1)} (P - \varepsilon S_{11})|_1 \, dy + \int_0^1 [-P\sigma_{1x} + \varepsilon S_{11}\sigma_{1x} - S_{12})]_{\sigma_1} \, dx +$$

$$- \int_0^1 [-P\sigma_{2x} + \varepsilon S_{11}\sigma_{2x} - S_{12})]_{\sigma_2} \, dx + \int_0^1 [\sigma_2 - \sigma_1] \, dx = 0. \tag{11}$$

while the second component becomes

$$\mathsf{Re} : \varepsilon^3\left(\int_0^1 dx \int_{\sigma_1}^{\sigma_2} \frac{dv}{dt} dy\right) = -\int_{\sigma_1(0)}^{\sigma_2(0)} (\varepsilon^2 S_{12})\big|_0 \, dy +$$

$$+ \int_{\sigma_1(1)}^{\sigma_2(1)} (\varepsilon^2 S_{12})\big|_1 \, dy + \int_0^1 \left[\varepsilon^2 S_{12}\sigma_{1x} + P - \varepsilon S_{12})\right]_{\sigma_1} dx +$$

$$- \int_0^1 \left[\varepsilon^2 S_{12}\sigma_{2x} + P - \varepsilon S_{12})\right]_{\sigma_2} dx + -\theta \int_0^1 [\sigma_2 - \sigma_1] \, dx = 0. \tag{12}$$

Condition (5) becomes

$$\int_0^h u(x, y, t) dy = 1. \tag{13}$$

4. The zero order approximation

Focussing on the zero-order approximation (that is neglecting all the terms containing ε) we find that in the viscous domain

$$\begin{cases} 0 = 1 - P_x + (S_{12})_y, \\ \\ 0 = -\theta - P_y, \\ \\ u_x + v_y = 0, \end{cases} \tag{14}$$

while in the rigid part

$$\begin{cases} u = k_1(t), \\ \\ v = \omega_2(t)x + k_2(t), \end{cases} \tag{15}$$

where $\omega_2(t)$ is the second order term in the expansion of the angular velocity

$$\omega = \underbrace{\omega_o}_{=0} + \underbrace{\omega_1}_{=0}\varepsilon + \omega_2\varepsilon^2 + ...$$

From $(14)_2$ we find that

$$P = -\theta y + P_o(x,t) + x, \tag{16}$$

where P_o is unknown.

Remark 3. *When writing (16) we are tacitly assuming that $P_o(x,t)$ is the same for both the domains $[0,\sigma_1]$, $[\sigma_2,h]$. This fact comes from the observation that the mechanical pressure is linear in y even in the unyielded domain. Indeed, let us go back to (8). Such equation holds also in the unyielded domain, where we know that*

$$II_S = \sqrt{S_{12}^2 + \frac{1}{2}\left(S_{11}^2 + S_{22}^2\right)},$$

and hence the components of $\mathbf{S}$*, are indeterminate but bounded. Hence, applying the lubrication scaling to the system (8) we find that equation $(8)_2$ reduces to $(14)_2$ also in the unyielded domain. As a consequence we write*

$$p\Big|_{[0,\sigma_1]} = -\theta y + P_{o1} + x,$$

$$p\Big|_{[\sigma_1,\sigma_2]} = -\theta y + P_{oY} + x,$$

$$p\Big|_{[\sigma_2,h]} = -\theta y + P_{o2} + x.$$

If we now impose the continuity of pressure across the yield surfaces σ_1, σ_2 we find

$$P_{o1} = P_{oY} = P_{o2},$$

which yields $P_o = P_{o1} = P_{o2}$.

The first component of the integral formulation of the plug momentum balance at the leading order reduces to

$$\int_{\sigma_1(0)}^{\sigma_2(0)} P|_0\, dy - \int_{\sigma_1(1)}^{\sigma_2(1)} P|_1\, dy + \int_0^1 \Big[(-P\sigma_{1x})|_{\sigma_1} + (P\sigma_{2x})|_{\sigma_2}\Big]dx +$$

$$+ \int_0^1 \Big[-S_{12}|_{\sigma_1} + S_{12}|_{\sigma_2}\Big]dx + \int_0^1 (\sigma_2 - \sigma_1)dx = 0. \tag{17}$$

while the second

$$\int_0^1 P|_{\sigma_1}dx - \int_0^1 P|_{\sigma_2}dx - \theta\int_0^1 (\sigma_2 - \sigma_1)dx = 0. \tag{18}$$

Because of (16) equation (18) is identically satisfied. From $(14)_1$ we find

$$P_{ox} = (S_{12})_y,$$

while, from (9), it is easy to check that at the leading order

$$S_{12} = u_y + \mathsf{Bi}\Big(\text{ sign } u_y\Big),$$

and

$$u_y + \mathsf{Bi}\Big(\text{ sign } u_y\Big) = P_{ox}y + c. \tag{19}$$

Because of the no-slip condition it is clear that we are looking for solutions such that

$$u_y > 0 \quad \text{ in } \quad (0,\sigma_1), \qquad\qquad u_y < 0 \quad \text{ in } \quad (\sigma_2,h),$$

and $S_{12}|_{\sigma_1} = \mathsf{Bi} = -S_{12}|_{\sigma_2}$. Integrating by parts equation (17) we find, after some algebra

$$-\int_0^1 P_{ox}(\sigma_2 - \sigma_1)dx = 2\mathsf{Bi}. \tag{20}$$

that is the equation of motion in the unyielded plug. On integrating (19) with classical no-slip conditions we get

$$\begin{cases} u = P_{ox}\left[\dfrac{(y-\sigma_1)^2 - \sigma_1^2}{2}\right], & y \in [0,\sigma_1] \\ \\ u = k_1(t), & y \in [\sigma_1,\sigma_2] \\ \\ u = P_{ox}\left[\dfrac{(y-\sigma_2)^2 - (h-\sigma_2)^2}{2}\right], & y \in [\sigma_2,h] \end{cases} \tag{21}$$

The requirement $u|_{\sigma_1} = u|_{\sigma_2}$ implies

$$\sigma_1^2 = (h-\sigma_2)^2 \qquad \Longrightarrow \qquad \sigma_2 = h - \sigma_1. \tag{22}$$

so that σ_2 is determined once σ_1 is determined[3]. Relation (22) shows that the unyielded plug is symmetric w.r.t. the centerline of the channel $y = h/2$. For simplicity of notation we set $\sigma = \sigma_1$. We have

$$k_1 = -\frac{P_{ox}\sigma^2}{2}. \tag{23}$$

Differentiating (23) w.r.t. x we find

$$P_{oxx}\sigma = -2P_{ox}\sigma_x. \tag{24}$$

[3]The solution $\sigma_1 = -(h-\sigma_2)$ has no physical meaning and it is therefore neglected

From the continuity equation $(14)_3$ and from the no-slip conditions we have

$$v\Big|_{\sigma} = -\int_0^{\sigma} u_x dy \qquad v\Big|_{h-\sigma} = \int_{h-\sigma}^{h} u_x dy.$$

Differentiating (21) w.r.t. x and plugging into the above we find

$$v\Big|_{\sigma} = \frac{\sigma^2}{6}\left[3P_{ox}\sigma_x + 2P_{oxx}\sigma\right] \tag{25}$$

$$v\Big|_{h-\sigma} = -\frac{\sigma^2}{6}\left[3P_{ox}\sigma_x + 2P_{oxx}\sigma + 3h_x P_{ox}\right]$$

Imposing $v|_{\sigma} = v|_{h-\sigma}$ we find

$$\frac{\sigma^2}{6}\left[6P_{ox}\sigma_x + 4P_{oxx}\sigma + 3h_x P_{ox}\right] = 0. \tag{26}$$

Plugging (24) into (26) we find

$$\frac{\sigma^2 P_{ox}}{6}\left[3h_x - 2\sigma_x\right] = 0,$$

yielding

$$3h_x = 2\sigma_x = -3A, \tag{27}$$

since $P_{ox} = 0$ or $\sigma = 0$ cannot be considered as solutions because would imply no flow.

Remark 4. *Plugging (24) into (25), (26) and exploiting (27) we get*

$$v\Big|_{\sigma} = -\frac{\sigma^2}{6}P_{ox}\sigma_x,$$

$$v\Big|_{h-\sigma} = -\frac{\sigma^2}{6}P_{ox}[3h_x - \sigma_x].$$

Exploiting (23) and (27) we find

$$v\Big|_{\sigma} = v\Big|_{h-\sigma} = \frac{k_1 h_x}{2},$$

so that, recalling $(15)_2$,

$$\frac{k_1 h_x}{2} = \omega_2 x + k_2. \tag{28}$$

As a consequence we conclude that the only admissible profiles of h are parabolic, linear and constant. Since we are dealing with a linear $h(x)$ we do not have to solve the problem at the order two to find ω_2 (which is unknown), since (28) automatically implies $\omega_2 = 0$. In the case of a parabolic h the problem at the order two should be solved to find the angular velocity ω_2. For simplicity we have focused on the linear case only.

Recalling that $v|_{\sigma} = \omega_2 x + k_2$, we can insert (24) into (25) and use (27) to find

$$-\frac{P_{ox}\sigma^2\sigma_x}{6} = -\frac{k_1 A}{2} = \omega_2 x + k_2. \tag{29}$$

which necessarily implies $\omega_2 \equiv 0$ and

$$2k_2 = -k_1 A.$$

Applying (13) we get

$$1 = \int_0^{\sigma} u dy + \int_{\sigma}^{h-\sigma} k_1 dy + \int_{h-\sigma}^{h} u dy,$$

and, after some algebra, we find

$$k_1 = \frac{3}{3h - 2\sigma}. \tag{30}$$

In conclusion we have found

$$\sigma = -\left(\frac{3A}{2}\right)x + K, \tag{31}$$

where K is unknown at this stage. We observe that the lower yield surface $y = \sigma$ is decreasing with x, whereas the upper yield surface $h - \sigma$ is increasing with x. In section 7, exploiting (20), we shall write an equation that allows to determine K in terms of A.

5. Constraints on K

To ensure the presence of the plug throughout the channel we must require

$$0 < \sigma(0) \leqslant h(0) - \sigma(0) \quad \Longleftrightarrow \quad 0 < \sigma(0) \leqslant \frac{1}{2},$$

$$0 < \sigma(1) < h(1) - \sigma(1) \quad \Longleftrightarrow \quad 0 < \sigma(1) < \frac{1 - A}{2},$$

The first condition ensures that the plug is present at the inlet of the channel. The second condition guarantees that the plug does not touch the channel walls at the outlet. Recalling (31) the above conditions become

$$\begin{cases} 0 < K < \dfrac{1}{2}, \\ \dfrac{3A}{2} < K < \dfrac{1}{2} + A. \end{cases} \tag{32}$$

The second of (32) makes sense only if

$$\frac{3A}{2} < \frac{1}{2} + A \quad \Longleftrightarrow \quad A < 1,$$

which is automatically satisfied because of (7). When $(32)_1$ is not satisfied, that is when

$$K > \frac{1}{2} \tag{33}$$

in an initial portion of the channel there is no plug. Indeed, when (33) holds $\sigma_1 > \sigma_2$ and the only portion in which $u_y = 0$ (and hence $S_{12} = \mathsf{Bi}$) is the center line $y = h/2$. In this case the onset of the plug occurs at some point $s \in (0, 1)$ and the region where the plug is present is $[s, 1]$. In the region $[0, s]$ the plug reduces to a set of zero measure constituted by the centerline $y = h/2$ only. The point s can be found imposing $h - \sigma = \sigma$. The latter yields $1 - As = -3As + 2K$, i.e.

$$s = \frac{2K - 1}{2A}. \tag{34}$$

where $s \in (0,1)$ when (33) and $(32)_2$ hold. Therefore our solution will be acceptable only if K satisfies

$$\frac{3A}{2} < K < \frac{1}{2} + A. \tag{35}$$

If $K < 1/2$ the plug exists in the whole channel. If $K > 1/2$ the plug starts at some point s given by (34).

6. The overall pressure drop

From (23) and (30) we find

$$P_{ox} = -\frac{6}{(3h - 2\sigma)}\frac{1}{\sigma^2}.$$

Recalling (31) and recalling that $h = 1 - Ax$ we find

$$P_{ox} = \frac{24}{(2K-3)(2K-3Ax)^2}. \tag{36}$$

From inequality (35) we notice that

$$\begin{cases} 2K - 3Ax \geq 2K - 3A > 0, \\ \\ 2K - 3 < 0, \end{cases} \tag{37}$$

since $A < 1$ and $x \in [0,1]$. Integrating (36) we determine the overall pressure drop

$$\Delta P = P\Big|_1 - P\Big|_0 = \frac{24}{2K-3}\int_0^1 \frac{dx}{(2K-3Ax)^2},$$

so that

$$\Delta P = \frac{12}{(2K-3)(2K-3A)K} < 0, \tag{38}$$

where $\Delta P < 0$ because of (37).

7. Tracking the yield surfaces

To track the position of the yield surfaces we go back to equation (20), that can be rewritten as

$$-\int_0^1 P_{ox}(h - 2\sigma)dx = 2\mathsf{Bi}.$$

Recalling (23) and (30), we get

$$2\mathsf{Bi} = \int_0^1 \frac{2k_1}{\sigma^2}(h-2\sigma)dy = \int_0^1 \frac{6(h-2\sigma)}{\sigma^2(3h-2\sigma)}dx.$$

Plugging (31) into the above we find

$$\int_0^1 \frac{1 - 2K + 2Ax}{(2K-3Ax)^2}dx = \frac{\mathsf{Bi}(3-2K)}{12}. \tag{39}$$

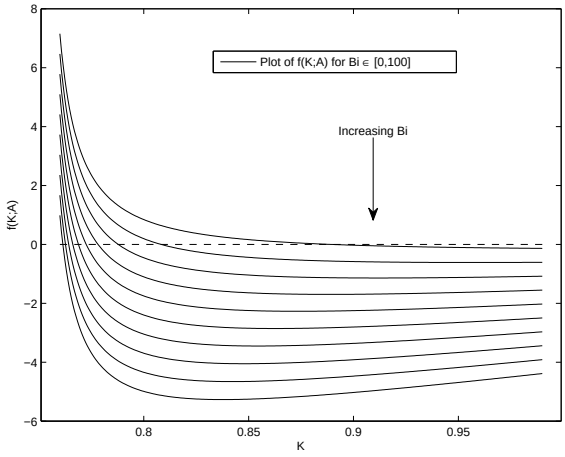

Figure 2: Plot of the function $f(K;A)$ for Bi ranging between 0 and 100.

which is the equation that must be solved to determine K. Since we are interested only in values of K that satisfies (35), we notice that, when (35) is met,

$$\begin{cases} 1 - 2K + 2Ax > 0, & \forall \quad x \in [0,1], \\ \\ 2K - 3Ax > 0, & \forall \quad x \in [0,1]. \end{cases}$$

Therefore, integration of (39) yields

$$f(K;A) = 0, \tag{40}$$

where

$$f(K;A) = \frac{2}{9}\ln\left[1 - \frac{3A}{2K}\right] + \frac{A(3-2K)}{6K(2K-3A)} - \frac{A\mathsf{Bi}(3-2K)}{12}. \tag{41}$$

The above is the implicit relation between A and K. Once K is found we get σ and $h - \sigma$, that is the yield surfaces separating the plug and the viscous phase.

To investigate the existence of a K satisfying $f = 0$ for a give A, we plot the function f with K in the range defined in (35) for different values of Bi for a fixed value of A. The plot in Fig. 2 shows the behavior of f as a function of K, for $A = 0.5$ and Bi ranging between 0 and 100. As one can notice for each value of Bi the function f has only one intersection with the K axis in the range specified, meaning that there exists a unique K satisfying (35). This can also be proved rigorously for any $A \in [0,1)$ and for each $\mathsf{Bi} \geqslant 0$. We refer to the appendix for the proof of such a statement.

8. Numerical examples

In this Section we consider some examples to illustrate the dependence of the yield surfaces σ, $h-\sigma$ and of the velocity (u,v) on the parameters A, Bi. Figs 3-6 show the position of the unyielded plug for

$$A = 0.1,\ \ 0.3,\ \ 0.5,\ \ 0.7, \qquad\qquad \mathsf{Bi} = 0.1,\ \ 5,\ \ 50.$$

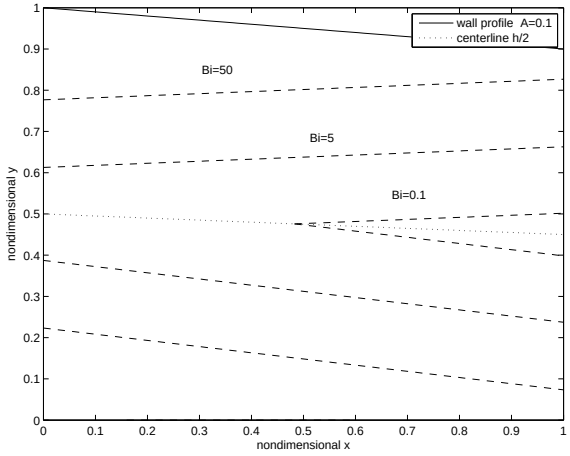

Figure 3: Plot of the unyielded plug for example 1 .

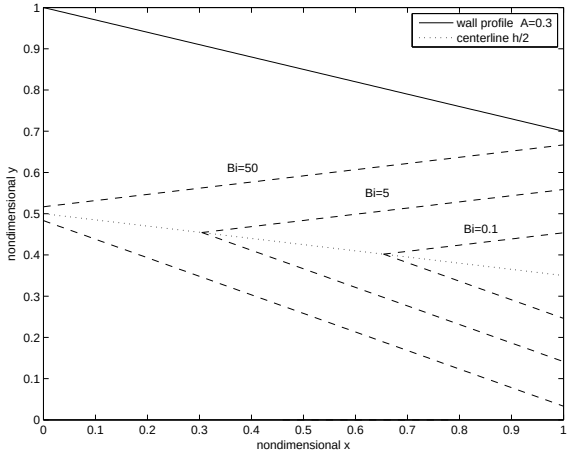

Figure 4: Plot of the unyielded plug for example 2 .

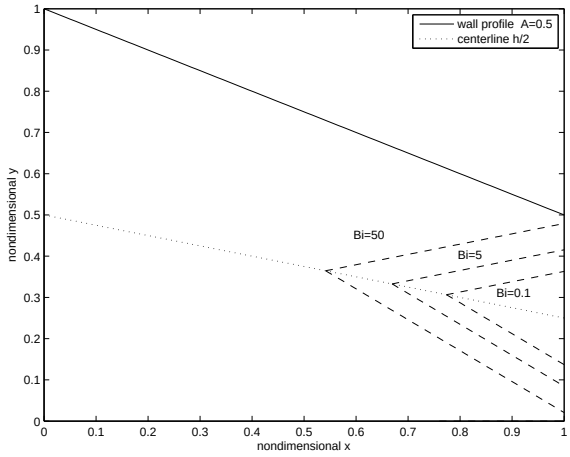

Figure 5: Plot of the unyielded plug for example 3 .

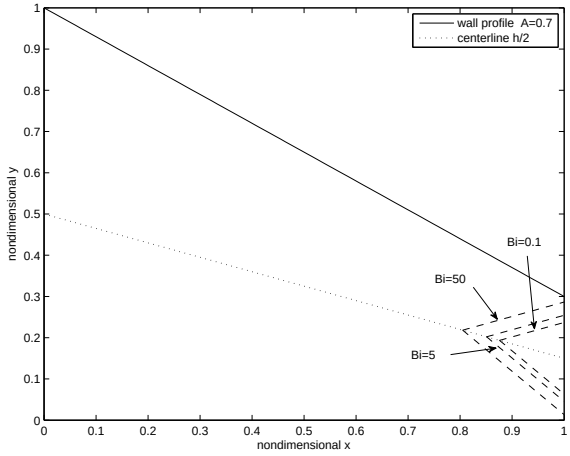

Figure 6: Plot of the unyielded plug for example 4 .

As one can easily realize, the larger is Bi, the larger is the region occupied by the unyielded part. On the other hand, when Bi is fixed, we observe that the unyielded part gets larger as the slope of the upper wall decreases. We also note that the onset of he unyielded part (which we recall is visible only for $K > 1/2$) is placed on the centerline $y = h/2$ as observed in Section 5.

In Fig. 7, 8 we have plotted the velocity components (u, v) for $\mathsf{Bi} = 5$ and $A = 0.3$. The plots display the components as function of y evaluated at $x = 0.4$, $x = 0.6$, $x = 0.8$. As one can see, the transversal component v is negative.

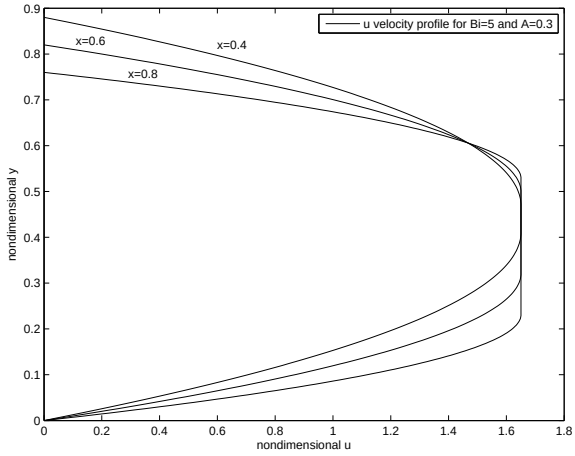

Figure 7: Plot of the longitudinal velocity u, $A = 0.3$, $\mathsf{Bi} = 5$.

9. Conclusions

We have studied the motion of a Bingham fluid in an inclined channel with flat, but not parallel, walls. The governing equation for the unyielded part has been obtained using a global integral approach introduced in [15], [16]. The advantage of this approach lies in the fact that no assumption has to be made

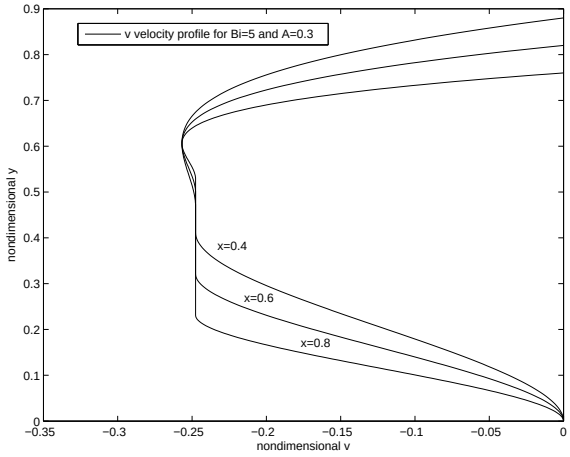

Figure 8: Plot of the transversal velocity v, $A = 0.3$, $\mathsf{Bi} = 5$.

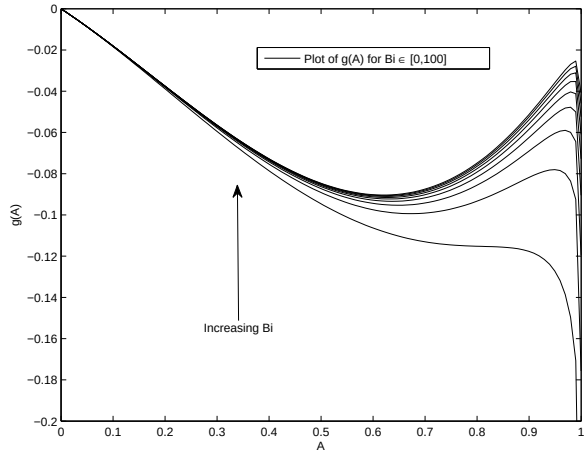

Figure A.9: Function $g(A)$.

.

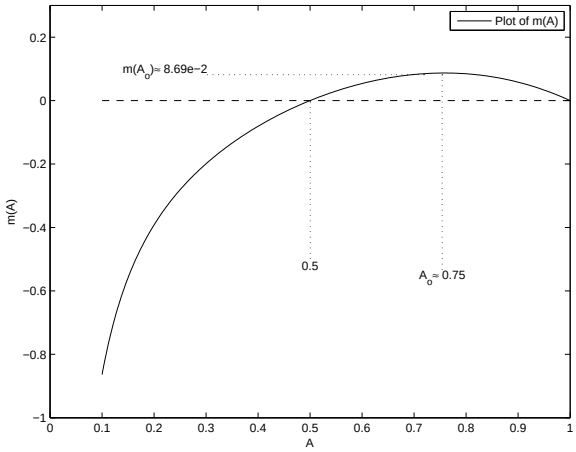

Figure A.10: Function $m(A)$.

on the order of magnitude of the stress components in the unyielded region.

We have studied the dynamics supposing that gravity is the only force driving the motion. Under the assumption of lubrication approximation, we have solved the problem, tracking the yield surface and determining constraints that prevent the flow from ceasing and that guarantee the existence of the plug. We have also determined an explicit formula for the pressure drop along the channel.

AppendixA. Mathematical analysis of equation (40)

We prove that, for any $A \in [0, 1)$ and for any $\mathsf{Bi} \geqslant 0$, there exists one and only one K fulfilling (40), with f given by (41). Indeed

$$\lim_{K \to (3A/2)^+} f(K; A) = \infty \qquad f(A, A + \frac{1}{2}) = g(A),$$

where

$$g(A) = \frac{4(2A+1)\ln\left(\dfrac{1-A}{1+2A}\right) + 6\mathsf{Bi}A^3 - 3\mathsf{Bi}A^2 + (12 - 3\mathsf{Bi})A}{18(2A+1)}$$

If we prove that $g(A) < 0$ for all $A \in (0, 1)$ and for all positive Bi, then, because of the continuity of $f(K; A)$, there exists "at least" one K such that $f(K; A) = 0$. We hence investigate the behavior of $g(A)$, whose plot for Bi ranging between 0 and 100 is shown in Fig. A.9. The function is negative, as expected, but we want to prove this result rigorously for any $A \in [0, 1)$ and for any $\mathsf{Bi} > 0$. We begin by noting that

$$g(0) = 0 \qquad \lim_{A \to 1^-} g(A) = -\infty.$$

We differentiate $g(A)$ w.r.t. A getting

$$g'(A) = \frac{\mathsf{Bi}(1-A)(2A-1)(2A+1)^2 - 12A}{6(1-A)(2A-1)^2} \qquad \text{(A.1)}$$

and we look for values A such that $g'(A) = 0$. These values are found solving

$$\frac{1}{\mathsf{Bi}} = \frac{(1-A)(2A-1)(2A+1)^2}{12A} =: m(A).$$

The plot of the function $m(A)$ is shown in Fig. A.10 As one can notice $m(A)$ has a maximum in $A_o \approx 0.75$ with $m(A_o) = 8.69 \cdot 10^{-2}$. As a consequence, when

$$\text{(Case I)} \qquad 0 \leqslant \mathsf{Bi}^{-1} < m(A_o)$$

there exist $1/2 \leqslant A_1 < A_o < A_2 \leqslant 1$, such that

$$g'(A_1) = g'(A_2) = 0$$

When

$$\text{(Case II)} \qquad \mathsf{Bi}^{-1} = m(A_o)$$

the only point where $g'(A)$ is null is A_o

$$g'(A_o) = 0$$

Finally, when

$$\text{(Case III)} \qquad \mathsf{Bi}^{-1} > m(A_o),$$

$g'(A)$ is always negative. In cases II, III it is trivial to check that $g(A) < 0$ for every $A \in [0, 1)$. In case I, the function $g(A)$ have a minimum in A_1 and a maximum in A_2. In particular $g(A_1) < 0$, since $g'(0) = -\mathsf{Bi}/6 < 0$. Suppose now that the maximum $g(A_2) > 0$. If this is the case, there exists some $\hat{A} \in (A_1, A_2)$ such that

$$g(\hat{A}) = 0, \qquad g'(\hat{A}) > 0. \tag{A.2}$$

Recalling the structure of $g(A)$, we see that $g(\hat{A}) = 0$ implies

$$\mathsf{Bi} = \frac{-12\hat{A} - 4(2\hat{A}+1)\ln\left(\dfrac{1-\hat{A}}{2\hat{A}+1}\right)}{6\hat{A}^3 - 3\hat{A}^2 - 3\hat{A}} \tag{A.3}$$

If we now insert (A.3) into (A.1) we find

$$g'(\hat{A}) = \frac{2\left[(2\hat{A}-1)(2\hat{A}+1)^2\ln\left(\dfrac{1-\hat{A}}{2\hat{A}+1}\right) + 3\hat{A}(\hat{A}-1)(4\hat{A}+1)\right]}{9\hat{A}(1-\hat{A})(2\hat{A}+1)^2}$$

Recalling that $1/2 < \hat{A} < 1$, it is easy to verify that the above expression implies $g'(\hat{A}) < 0$, which is in clear contradiction with $(\text{A.2})_2$. We have therefore proved that the function $g(A) < 0$ for all $A \in (0, 1)$ and for all $\mathsf{Bi} > 0$.

So far we have proven that there exists at least one solution K such that $f(K; A) = 0$, with K satisfying (35) and for each $A \in [0, 1)$. Now we prove that such a solution is unique. To this aim we consider the derivative of f w.r.t. K

$$\frac{\partial f}{\partial K} = \frac{A\left[\mathsf{Bi}(4K^4 - 12AK^3 + 9A^2) + 12K(K - A - 1) + 9A\right]}{6K^2(2K-3A)^2}.$$

Suppose that $\hat{K}$ is one solution whose existence has been proved, so that $f(\hat{K}; A) = 0$. Recalling the definition of f we find, after some algebra,

$$\mathsf{Bi} = -\frac{2\left[4\hat{K}\left(2\hat{K}-3A\right)\ln\left(1-\dfrac{3A}{2\hat{K}}\right) + 3A(3-2A)\right]}{3A\hat{K}(2\hat{K}-3)(2\hat{K}-3A)}$$

On substituting into $\partial f/\partial K$ we find

$$\left.\frac{\partial f}{\partial K}\right|_{\hat{K}} = \frac{f_1 + f_2}{f_3},$$

where

$$f_1 = 8\hat{K}^2(2\hat{K}-3A)\ln\left(1-\frac{3A}{2\hat{K}}\right),$$

$$f_2 = 3A(3-2\hat{K})(16\hat{K}^2 - 18A\hat{K} - 12\hat{K} + 9A),$$

$$f_3 = 18\hat{K}^2(3-2\hat{K})(2\hat{K}) - 3A)^2.$$

Recalling that

$$\frac{3A}{2} < \hat{K} < A + \frac{1}{2} < \frac{3}{2}$$

it is trivial to see that $f_1 < 0$, $f_3 > 0$. For what concerns f_2 we need to determine the sign of the parabola

$$\ell(K) = 16K^2 - 18AK - 12K + 9A.$$

Simple calculation shows that the roots K_1, K_2 of $\ell(K)$ are real for every value of A. In particular, it is easy to verify that

$$K_1 < \frac{3A}{2} < A + \frac{1}{2} < K_2,$$

so that

$$\ell\Big|_{\left[\frac{3A}{2}, A+\frac{1}{2}\right]} < 0 \qquad \Longrightarrow \qquad f_2 < 0.$$

In conclusion we have proven that

$$\left.\frac{\partial f}{\partial K}\right|_{\hat{K}} < 0. \tag{A.4}$$

Inequality (A.4) must hold for every solution $\hat{K}$ and this clearly implies that the solution $\hat{K}$ has to be unique.

[1] Balmforth N.J., Craster R.V., A consistent thin-layer theory for Bingham fluids, J. Non-Newt. Fluid Mech. **84** (1999) 65–81.

[2] Balmforth N.J., Frigaard I.A., Ovarlez G., Yielding to stress: recent developments in viscoplastic fluid mechanics, Annu. Rev. Fluid Mech. (2014) 121–146.

[3] Bingham E.C., An Investigation of the Laws of Plastic Flow, U.S. Bureau of Standards Bulletin, 13, (1916) 309-353.

[4] Bingham E.C., Fluidity and Plasticity, McGraw Hill (1922).

[5] Bird R.B., Stewart W.E., Lightfoot E.N., Transport Phenomena, Wiley (1960).

[6] Frigaard I.A., Ryan D.P., Flow of a visco–plastic fluid in a channel of slowly varying width, J. Non-Newt. Fluid Mech., 123, (2004) 67–83.

[7] Fusi L., Farina A., An Extension of the Bingham Model to case of an Elastic Core, Advances in Mathematical Sciences and Applications, Vol. 13, N.1, (2003), 113-163.

[8] Fusi L., Farina A., A Mathematical Model for Bingham-like Fluids with Visco- Elastic Core, Z. angew. Math. Phys. (Journal of Applied Mathematics and Physics), Birkhuser Verlag AG, Vol. 55 (5), (2004), 826-847.

[9] Fusi L., Farina A., Modelling of bingham-like fluids with deformable core, Computers & Mathematics with Applications, Vol. 53, 3-4,(2007), 583-594.

[10] Fusi L., Farina A., A Mathematical model for an upper convected Maxwell fluid with an elastic core: study of a limiting case, International Journal of Engineering Science, Vol. 48 , N. 11, (2010), 1263-1278.

[11] Fusi L., Farina A., Pressure-driven flow of a rate type fluid with stress threshold in an infinite channel, International Journal of Nonlinear Mechanics, Vol. 46, (8), (2011), 991-1000.

[12] Fusi L., Farina A., Rosso F., Flow of a Bingham-like fluid in a finite channel of varying width: A two-scale approach, J. Non-Newt. Fluid Mech., 177-178, (2012), 76–88.

[13] Fusi L., Farina A., Rosso F., The Lubrication Paradox for the Flow of a Bingham Fluid on a Inclined Surface, International Journal of Non-Linear Mechanics, 58, (2014), 139–150.

[14] Fusi L., Farina A., Rosso F., Retrieving the Bingham model from a bi-viscous model: Some explanatory remarks, App. Math. Lett., 27, (2014), 11–14.

[15] Fusi L., Farina A., Rosso F., Roscani S., Pressure Driven Lubrication Flow of a Bingham Fluid in a Channel: A Novel Approach, J. Non-Newt. Fluid Mech., 221, (2015), 66-75.

[16] Fusi L., Farina A., Rosso F., Planar squeeze flow of a bingham fluid, Journal of Non-Newtonian Fluid Mechanics 225 (2015), 1–9.

[17] Lipscomb G.G., Denn M.M., Flow of Bingham fluids in complex geometries, J. Non-Newt. Fluid Mech., **14** (1984) 337–346.

[18] Muravleva L., Squeeze plane flow of viscoplastic Bingham material, J. Non-Newt. Fluid Mech., **220** (2015) 148–161.

[19] Oldroyd S.G., A rational formulation of the equation of plastic flow for Bingham solid, Proc. Cambridge Philos. Soc., 45 (1947) 100–105.

[20] Putz A., Frigaard I.A., Martinez D.M., On the lubrication paradox and the use of regularisation methods for lubrication flows, J. Non-Newt. Fluid Mech., 163, (2009) 62–77.

[21] Rajagopal K.R., On implicit constitutive theories, Appl. Math., 48, (2003) 279–319.

[22] Rajagopal K.R., On fully developed flows of fluids with a pressure dependent viscosity in a pipe, Appl. Math., **50**, (2005), 341–353.

[23] Rajagopal K.R., On implicit constitutive theories for fluids, J. Fluid Mech., 550, (2006) 243–249.

[24] Rajagopal K. R., Saccomandi G., Vergori L., Flow of fluids with pressure and shear-dependent viscosity down an inclined plane, J. Fluid Mech., 706 (2012) 173-189.

[25] Roussel N., Lanos C., Plastic fluid flow parameters identification using a simple squeezing test, Appl. Rheol. **13** (2003) 132-141

[26] Walton I.C., Bittleston S.H., The axial flow of a Bingham plastic in a narrow eccentric annulus, J. Fluid Mech., **222**, (1991) 39–60.

[27] Wilson S.D.R., Squeezing flow of a Bingham material, J. Non-Newt. Fluid Mech., **47** (1993) 211–219.